Micro and Nanostructures 187 (2024) 207769

Contents lists available at ScienceDirect

Micro and Nanostructures

journal homepage: www.journals.elsevier.com/micro-and-nanostructures

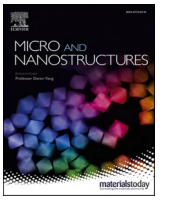

A python implementation based lattice Boltzmann method for thermal behavior analysis in silicon carbide MOSFET

Khaled Mansouri [a], Oussama Zobiri [a], Abdelmalek Atia [a,b,*], Müslüm Arıcı [c]

[a] LEVRES Lab, University of El Oued, Technology Faculty, 39000, El Oued, Algeria
[b] UDERZA Unit, University of El Oued, Technology Faculty, 39000, El Oued, Algeria
[c] Mechanical Engineering Department, Engineering Faculty, Kocaeli University, 41001, Kocaeli, Turkey

ARTICLE INFO

Keywords:
Lattice Boltzmann method
SiC MOSFET
Hotspot
Specularity parameter
Python implementation

ABSTRACT

In the new global industrial sector, electronics systems efficiency has become a central issue should be improved. Recently, there has been renewed interest for addressing this challenge by integrating Silicon Carbide (SiC) technology in industrial systems due to its outstanding materials properties compared to other used material. Meanwhile due to continue minimization of the scale of electronic devices, SiC MOSFETs are highly affected by thermal behavior, a major issue that requires further scientific investigation. In this paper, a Python code-based Lattice Boltzmann Method is implemented to characterize the thermal behavior inside a SiC MOSFETs. The aim of this essay is to explore the relationship between the hotspot and the specularity parameter which is the probability of phonons scattering in the considered nano structure. What emerges from the results reported in this work is that there is an association between the reduction of hotspots inside Silicon Carbide MOSFET and the augmentation of specularity parameter. For $R_{th}^{-1} = 10^8$ W/(m^{2}K) and specularity parameter of 0.7 and 0.3, the temperature difference was 1.74 K and 1.95 K, respectively while it was 1.21 K and 1.47 K for $R_{th}^{-1} = 10^{10}$ W/(m^{2}K) at the same specularity parameters.

1. Introduction

The continuous attention about the importance of industrial electronics has driven to intensive scientific investigation in the field of transistor performances enhancement. Over the past century, there has been a dramatic increase in the utilization of power electronics devices. Nowadays, there is a growing of many studies that recognize the importance of using semiconductor-based Silicon Carbide in different electronic systems due to many benefits [1]. It leads to important advantages such as (1) decreasing the volume and masse of switch, (2) improvement of the cost effectiveness of the photovoltaic energy output and (3) to play a pivotal role in minimizing the energy loss and maximizing the efficiency and countability [2,3].

Ding et al. [3] investigated the effects of SiC MOSFETs on the inverter used in low-voltage microgrid performances such as efficiency and power quality output. A double pulse test is used to assess the properties of SiC and Si while taking into account thermal effects. On the basis of the double pulse test (DPT) results at various temperature, the authors computed the switching losses and conduction. The tested switching and thermal conduction parameters of SiC are also utilized to estimate the phase voltage distortions, which yield harmonic components related to phase current. A study compared between Si IGBTs and SiC MOSFETs considering

* Corresponding author. LEVRES Lab, University of El Oued, Technology Faculty, 39000, El Oued, Algeria.
E-mail addresses: khaled-mansouri@univ-eloued.dz (K. Mansouri), abdelmalek-atia@univ-eloued.dz (A. Atia).

https://doi.org/10.1016/j.micrna.2024.207769
Received 3 November 2023; Received in revised form 28 December 2023; Accepted 21 January 2024
Available online 24 January 2024

variations in their junction temperatures in a PV solar inverter [4]. By entering the current mission trends that were taken from a photovoltaic power plant over the course of a year into a computation tool, these variances are estimated. The latter is based on a thermal model with a link between a loss model and a thermal model. The findings showed that the semiconductor temperature consent for the identification and comparison of thermal restrictions in SiC transistor and Si device PV modules. Öztürk et al. [5] examined a practical design of SiC converter in PV connected grid. They found that Silicon Carbide MPPT converter has an efficiency improvement reached to 1.7 % compared to Si-IGBT MPPT converter. A design tool has been introduced by Sintamarean et al. [6] for testing the practical SiC photovoltaic inverter reliability in Arizona state, USA. This study took into account field operation conditions throughout a year. The results show that there is a significant impact on the expected converter lifetime where the SiC PV-inverter is running. The degradation mechanism of 1.2 kV Silicon Carid MOSFET and 1.2 kV Si IGBT under the same power cycling test was estimated [7]. In this study, the trends of both electrical and thermal behavior are analyzed comparatively between two devices. The obtained results showed that the Silicon Carid MOSFET fails earlier than Silicon IGBT device, and SiC MOSFET presented better performances in comparison with Si IGBT. This study emphasizes the need for more investigation of SiC transistor in terms of thermal and electrical characteristics.

Nowadays, industry and any other application such as photovoltaic conversion system requires smaller size and portable devices thanks to the transistor's size shrank from the macro-scale to the nano scale, enabling an exponential increase of semiconductor number in electronic systems [8]. The silicon-based subsurface layer typically has many benefits. However, the issue of self-heating and its implications on the related system has been a controversial and much disputed subject within this field [9]. Power modules with silicon carbide (SiC) transistors are very appealing products that are already on the market. However, despite advancements in technology, reliability is still a problem, necessitating reliability assessments before these devices are widely used in power systems [10]. Kim and Funaki [11] described a method for measuring unsteady heat conduction resistance and performing thermal investigation on packed SiC MOSFETs. A constant current measurement of the relationship between a MOSFET's gate-source voltage and temperature is performed. This work is conducted under a heating state using a current injection of 2 A. The yields of the current work in terms of thermal resistance are compared to those obtained via finite difference method, the comparison indicates good agreement between both results. The Short-circuit periods leads to fail the MOSFET devices catastrophically due successive self-heating.

The majority of existing studies on thermal behavior analysis within semiconductors devices used conventional methods such as finite element method (FEM) [12]. Meanwhile, it should bear in mind that the FEM is based on macroscale models such as single phase lag that were derived using thermal energy equation [13]. The potential problem associated with the scope of these models is the requirement of some modification on the heat equation by adding other terms to follow the thermal trends inside nanoscale MOSFET [14]. To solve this problem, lattice Boltzmann method was proposed due to its powerful to deal phonon transport within nano scale structures [15]. This method gives more closely results compared to available experimental data in literatures because it considers both short temporal and spatial scales effects [16]. The present study aims to investigate nano thermal phonon transport within Silicon Carbide MOSFET via the utilization of Lattice Boltzmann method. The role of Robin boundary condition and specularity parameter on thermal behavior are presented in the current work. The used mesoscopic model does not require any modification on mathematical model to examine the thermal propagation and its impact within the nano MOSFET based SiC material.

2. Lattice Boltzmann methodology

A considerable amount of literature has been published on Lattice Boltzmann Method (LBM) [17,18]. These studies reveal the importance of LBM in the era of computational fluid dynamics (CFD) due to its numerous advantages, such as the easier implementation of complex geometry and boundary condition, simplicity programming and coupling with machine learning algorithms to enhance the results yields from CFD. In the case of nano-thermal conduction, The LB method is one of the more practical ways of photon radiation modelling and simulation [19]. The present study utilizes the phonons Boltzmann equation with single relaxation time approximation. The adopted approach uses statistical analysis in order to gain insights into phonons distributions and their energy density development:

$$\frac{\partial g}{\partial t} + v.\nabla g = -\frac{g - g^{eq}}{\tau_b} + q_v \tag{1}$$

The present study utilizes Debye formulation to define the relationship between the density of energy and temperature [16]:

$$g(T) = \left(\frac{9\eta k_B}{\theta^3}\int_0^{\theta/T}\frac{o^3}{e^o - 1}dz\right)T^4 \tag{2}$$

in this equation, θ is the Debye temperature is the temperature of a particle's highest normal mode of vibration., o signifies the dimensionless variable, and η indicates the density oscillator is parameter used for investigating the fundamental mechanisms of relaxation oscillators.

Owing to nano dimension, the heat diffusion process is yielded by phonons vibration [20]. The following equation is intended to define the effective thermal conductivity:

$$k_e = k\left[1 - \frac{2 \times Kn \times \tanh(1/(2 \times Kn))}{1 + c \times \tanh(1/(2 \times Kn))}\right] \tag{3}$$

Here, c can be described as a variable connects with the type of material and it estimates as $c = 2(1+p)/(1-p)$ where p is the specularity parameter [21]. The term 'τ_b' is defined as the relaxation time, it is used to refer the phonons scattering process [22]:

$$\tau_b = \frac{3 \times k_e}{C \times v^2} \tag{4}$$

The discretization step of the Boltzmann model produces a network, most commonly a square model. As explained earlier, the discretized Boltzmann equation is expressed as:

$$g_i(r + \Delta r_i, t + \Delta t) - g_i(r,t) = -\frac{\Delta t}{\tau_b}[g_i(r,t) - g_i^{eq}(r,t)] + w_i \Delta t q_v \tag{5}$$

Here, Δt, w_i and Δr are the time step, weighting factor and space step, respectively. Fig. 1 presents the LBM model.
The total energy density is presented as:

$$g(r,t) = \sum_{i=1}^{8} g_i(r,t) = \sum_{i=1}^{8} g_i^{eq}(r,t) \tag{6}$$

The equilibriem distribution function can presented as follow:

$$g_i^{eq}(r,t) = \frac{1}{8} g(r,t) \tag{7}$$

The dimensionless terms are used for simplification and linking between variables for calculation. The nondimensionalizes equation were normalized using the following terms:

$$g^* = \frac{g - g_{ref}}{g_{ref}}, t^* = \frac{t}{\Delta t}, r^* = \frac{r}{\Delta r}, T^* = \frac{T - T_{ref}}{T_{ref}}, q_v^* = \frac{\Delta t \times q_v}{C \times T_{ref}} \tag{8}$$

The dimensionless state of Eq. (5) can be rewritten as:

$$g_i^*(r^* + \Delta r^*, t^* + \Delta t^*) - g_i^*(r^*, t^*) = -\frac{\Delta t^*}{\tau_b^*}[g_i^*(r^*, t^*) - g_i^{eq*}(r^*, t^*)] + w_i q_v^* \tag{9}$$

3. Computational domain description

The design of nano-structure transistor is represented in Fig. 2. In this work, the structure has a dimensions of L = 100 nm, the graphene material thickness is 0.35 nm and $l = 50$ nm [23]. The simulation work is carried out using a constant internal thermal ($q_v = 10^{19}$ W/m^3). A temperature jump boundary condition is employed at the interface phonon-wall, it formulated as [23,24]:

$$T - T_w = -d \times Kn \times L_c \frac{\partial T}{\partial y} \tag{10}$$

in this equation, d and Kn referred the Knudsen number which is a dimensionless number defined as the ratio of the particle mean free

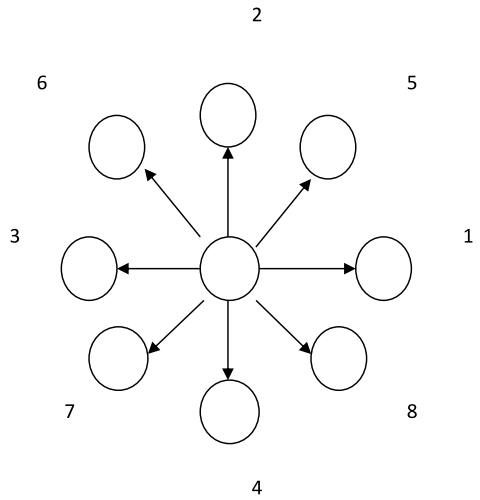

Fig. 1. D_2Q_8 LBM model.

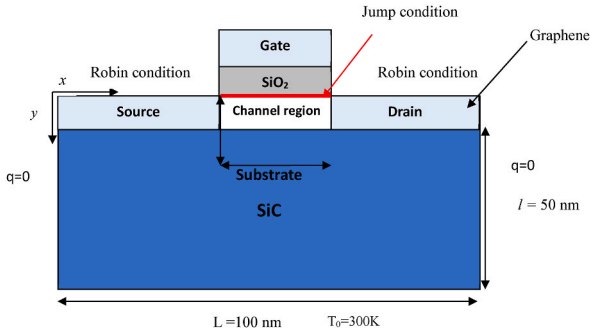

Fig. 2. Graphene MOSFET based on SiC substrate schematic.

path length to a representative physical length scale.

The Dirichlet condition approach was adopted at the bottom layer to ensure that the temperature is constant (300 K). The right and left sides of the studied system are considered to be isolated (adiabatic). At t = 0, the temperature of MOSFET device is supposed to be around 300 K. One of the most well-known tools for assessing the role of convection at top layer (source/drain) is the employment of Robin boundary condition, it's expressed as follow [25]:

$$-k_e\frac{\partial T}{\partial y}=\frac{(T-T_0)}{R_{th}}=h(T-T_0) \tag{11}$$

4. Simulation results and discussion

The current study reports on the 2D heat conduction inside transistor devices based on carbide silicon substrates using the D2Q8 Lattice Boltzmann model, the mixed type of boundary condition and effective thermal conductivity are considered. Table .1 lists the parameters and attributes of graphene and carbide silicon used in the numerical simulation. The convective thermal coefficient values are $h = R_{th}^{-1} = 10^{10}$ W/(m^{2}K) and 10^8 W/(m^{2}K) [25]. An important implementation in the present paper is the use of high-level programming language (Python 3.11). We implement LBM and solve the problems in a single Graphics Processing Unit. Fig. 3 depicts the steps informatics operation chart, where Python code is used to describe the transfer of heat inside nanoscale device. Fig. 4 shows temperature difference (T-Tref) trends at midline of the nano transistor device with time between the current study and other models. The outputs of current model which is nano-graphene transistor devices based on carbide silicon substrate are compared with Ballistic Diffusive Equation (BDE), Boltzmann Transport Equation (BTE), Fourier law in Ref. [26] and Single Phase Leg (SPL) model in Ref. [24] which is used a silicon material on design nano-MOSFET. The yields in this investigation were compared to those of other studies in terms of augmenting hotspot. In addition, what stands out in this figure is the decreasing of temperature difference with the augmentation of inversed thermal resistance. The observed difference could be attributed to thermal convection enhancement. The temperature rise produced by SiC and Si materials is highlighted in Table 2. Interestingly, a significant difference was observed from this comparison. An alternative explanation for this result is that it could be due to high thermal conductivity of silicon carbide material compared to Silicon material. Fig. 5 exhibits the comparison between the findings of the present study and those reported in literature in terms hotspot difference according to y direction, at scalable time of t = 10 ps and centerline of x direction. In the models of BDE [27], SPL [24] and Double Phase Leg (DPL) [13] high hotspots are detected at interfaces. The collision rate at the contact wall is responsible for the disparity in curves and values with the materials used in the design of the devices, where in our current model, graphene and silicon carbide were used as a substrate, but in other models, silicon was used in the design of the MOSFET device due to knowing that silicon is less thermal conductive compared to the other two materials. Fig. 6 depicts the influence of specularity parameter on the convective coefficient at t = 40 ps in a nano-graphene device (current model). The growth of hotspot with the dropping of the specularity parameter is evident in figure. A possible explanation for this might be the impact of specularity parameter on occasional collisions at the boundary of the nano device in question. What stands out in this figure is the rapid increase of heat exchange at early time. The temperature difference is valued respectively as 1.74 K and 1.95 K for $p = 0.7$ and 0.3 for the case of $R_{th}^{-1} = 10^8$ W/(m^{2}K), while the yields for $R_{th}^{-1} = 10^{10}$ W/(m^{2}K) are 1.21 K and 1.47 K for p = 0.7 and 0.3, respectively. The small temperature differences are importance to pass the electrical current smoothly without the effect of the relevant heat. Fig. 7 demonstrates the heat difference along the y-axis of a nano-transistor for different specularity values and convective heat transfer coefficients at t = 20 and 40 ps. The maximum hotspot is obviously found at the interface. Furthermore, for $R_{th}^{-1}=10^{10}$ W/(m^{2}K), the temperature decreases,

Table 1
Properties of silicon carbide (SiC) and graphene (Gr).

/	Λ (nm)	v (m/s)	C (J/m^{3}K)	k (W/m·K)
Gr	518	14740	1.57×10^6	4000
SiC	53	13000	2.11×10^6	490

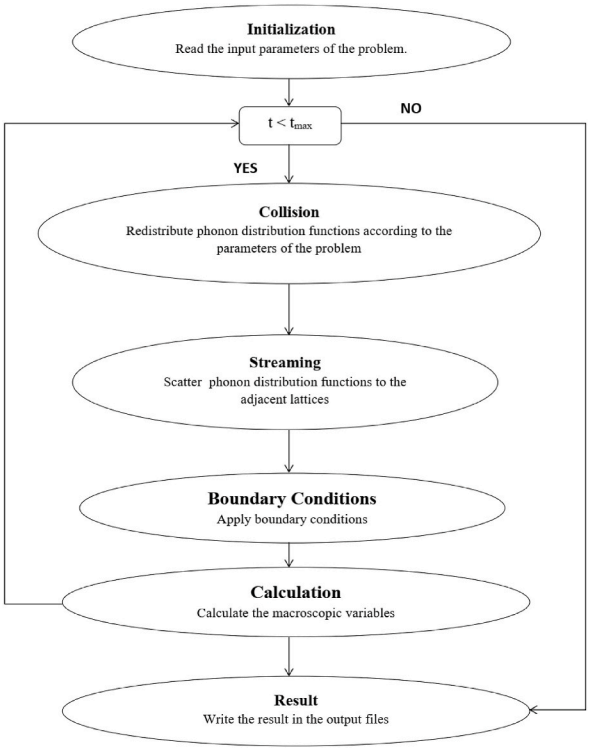

Fig. 3. Simulation chart.

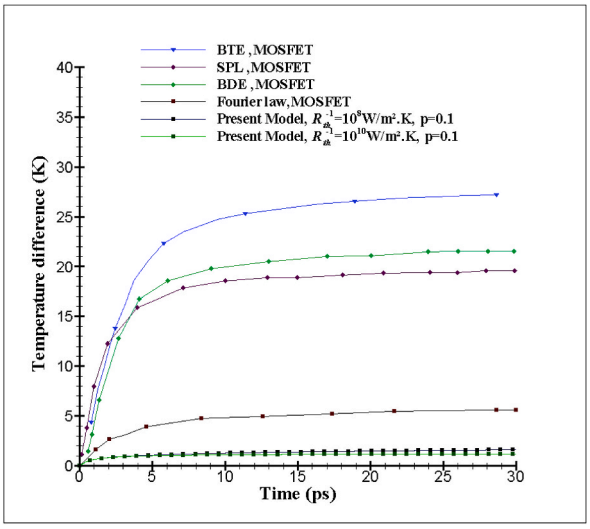

Fig. 4. The variation of temprature difference with time at the centerline between prsent model and other models.

Table 2
Temperature difference comparison between SiC MOSFET and Si MOSFET at 30 ps.

Study	Yang et al. [26]	Yang et al. [26]	Yang et al. [26]	Nasri et al. [24]	Present study
Material	Si	Si	Si	Si	SiC
Model	BTE	BDE	Fourier law	SPL	LBM
T-Tref	27 K	21.3 K	5.3 K	19.5 K	1.7 K

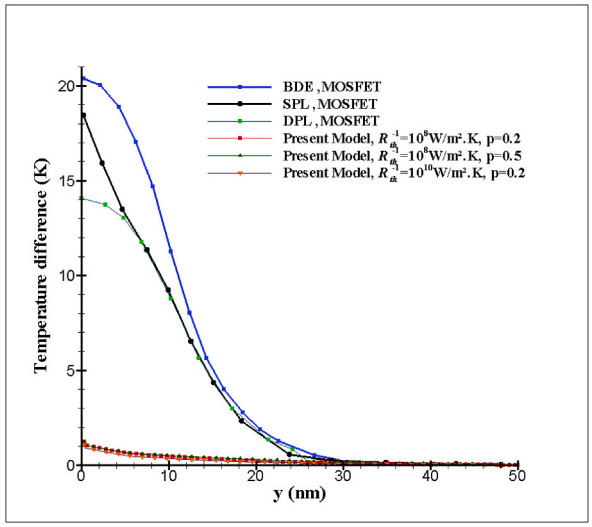

Fig. 5. The variation of temprature difference according to *y* axis between present model and other models.

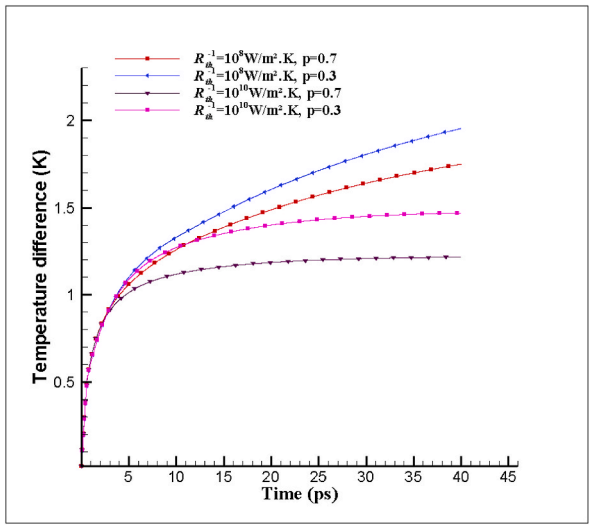

Fig. 6. The variation of temprature difference at the centerline virsus time.

demonstrating the efficient component of this term to reduce heat. The curves overlap due to changes in the value of the convection coefficient and the thermal conductivity associated to the specularity coefficient. The difference in heat flow beside the midline of the examined device at various convective coefficients and times is depicted in Fig. 8. Because of the heat generated by the collision at the interface wall - phonon, high values of heat flow are seen at the boundary for all statuses, and heat flow increases with time, reaching 21.11×10^{10} and 23.86×10^{10} W/m^2 at scaled times of t = 20 and 40 ps, respectively. When the convection coefficient is adjusted to $R_{th}^{-1} = 10^{10}$ W/(m^{2}K) at t = 20 and 40 ps, the heat flow decreases (19.83×10^{10} W/m^2 and 20.45×10^{10} W/m^2). This thermal decrease is caused by the reduce of heat at the drain and source. The impacts of convective coefficients and specularity parameters on two-dimensional hotspot distribution in a nano-device at different times are shown in Fig. 9. The shape of the heat distribution differs between the figures due to the effect of the convective coefficients and specularity parameters, whereas significant hotspot values are observed in the zone active where the collision wall-phonon is present. The hotspot distribution is observed for $R_{th}^{-1} = 10^{10}$ W/(m^{2}K) while the heat flux is retrieved by the convective coefficient formulated by the mixed type boundary condition at the top of the source drain.

5. Conclusions

Due to the importance of thermal behavior understanding and management inside the SiC MOSFET for PV system, the aim of the

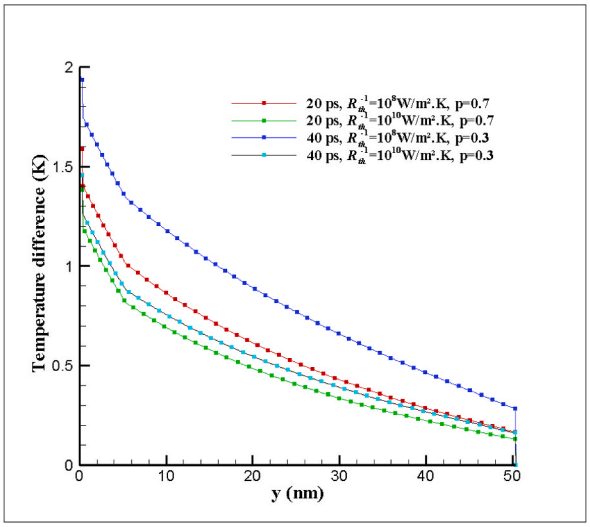

Fig. 7. The variation of temprature difference at different times.

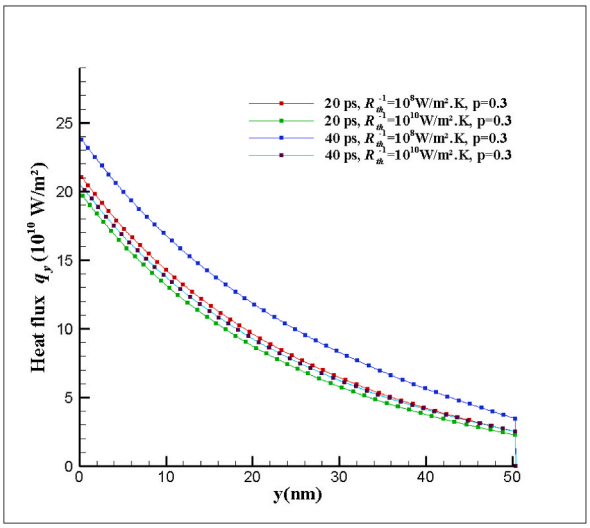

Fig. 8. Thermal flux trends according *y* axis at cenreline of SiC Mosfet (x = L/2).

current paper was to examine the credibility of nanoscale graphene MOSFET based on SiC substrate material. A python code based on Lattice Boltzmann model is developed to investigate the thermal behavior taking into account the specularity parameters (p) and applying convective boundary condition. For $h = R_{th}^{-1} = 10^{10}$ W/(m^{2}K), The temperature difference reached to 1.21 K and 1.47 K for p = 0.7 and 0.3, respectively. The results of this study indicate that the hotspots distribution is symmetrical at centerline axis centerline. In addition, the heat flux trend occurred with successive increases in time, in which it reached respectively to 211.1 and 238.6 GW/m^2 at t = 20 and 40 ps. Another important finding is the decrease of heat flux (204.5 GW/m^2 and 198.3 GW/m^2) was indicated when the factor of thermal convection is increased. One of the more significant yields to appear from this work is that the specularity parameters contributes well for reducing the hotspots inside the nano-transistors in question. The research has also shown that the same conclusion for convective coefficient. The second major finding was that the silicon carbide MOSFET presented more thermal stability compared to other types of nano transistor. A further study could assess the long-term effects of thermal transport in SiC MOSFET is needed to be analyzed via 3D lattice Boltzmann method considering electrical term with non-uniform thermal sources.

CRediT authorship contribution statement

Khaled Mansouri: Software, Validation, Visualization. **Oussama Zobiri:** Conceptualization, Formal analysis, Methodology, Writing – original draft. **Abdelmalek Atia:** Investigation, Methodology, Project administration, Writing – review & editing. **Müslüm**

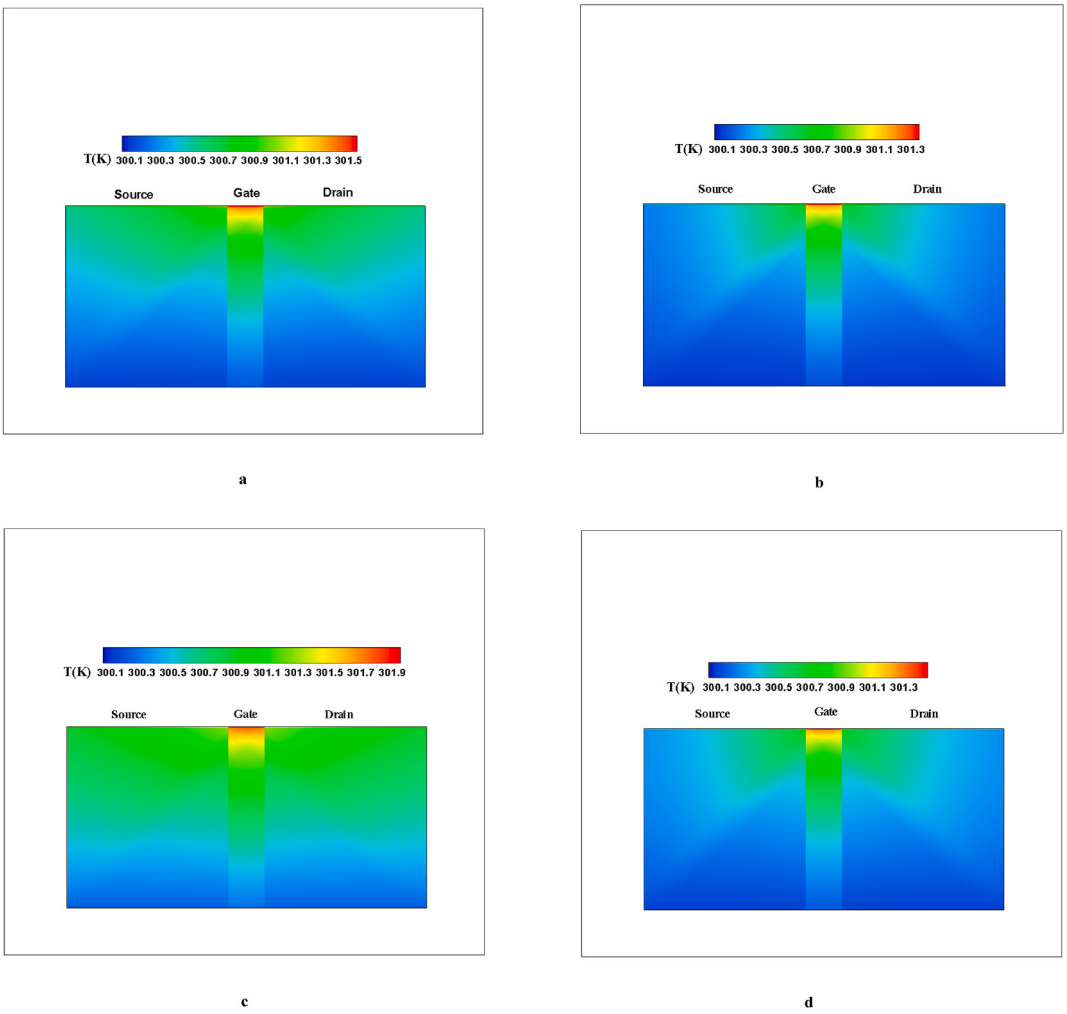

Fig. 9. 2D isothermal distribution within SiC MOSFET: a) $h = 10^8$ W/(m^2.K), $p = 0.7$ and t = 20 ps ; b) $h = 10^{10}$ W/(m^2.K), $p = 0.7$ and t = 20 ps; c) $h = 10^8$ W/(m^2.K), $p = 0.3$ and t = 40 ps and d) $h = 10^{10}$ W/(m^2.K), $p = 0.3$ and t = 20 ps.

Arıcı: Supervision, Writing – review & editing.

Declaration of competing interest

We wish to confirm that there are no known conflicts of interest associated with this publication. Also, we declare that this manuscript is original, has not been published before and is not currently being considered for publication elsewhere and it has been read and approved by all named authors.

Data availability

No data was used for the research described in the article.

Acknowledgment

The current research is supported by the DZ general directorate of scientific research and technological development.

References

[1] A. Pérez-Tomás, P. Godignon, N. Mestres, J.J.M.e. Millán, A field-effect electron mobility model for SiC MOSFETs including high density of traps at the interface, Microelectron. Eng. 83 (2006) 440–445, https://doi.org/10.1016/j.mee.2005.11.007.

[2] B.N. Pushpakaran, A.S. Subburaj, S.B. Bayne, J.J.R. Mookken, S.E. Reviews, Impact of silicon carbide semiconductor technology in Photovoltaic Energy System, Renew. Sustain. Energy Rev. 55 (2016) 971–989, https://doi.org/10.1016/j.rser.2015.10.161.
[3] X. Ding, F. Chen, M. Du, H. Guo, S.J.A.E. Ren, Effects of silicon carbide MOSFETs on the efficiency and power quality of a microgrid-connected inverter, Appl. Energy 201 (2017) 270–283, https://doi.org/10.1016/j.apenergy.2016.10.011.
[4] M. Dbeiss, Y. Avenas, H.J.M.R. Zara, Comparison of the electro-thermal constraints on SiC MOSFET and Si IGBT power modules in photovoltaic DC/AC inverters, Microelectron. Reliab. 78 (2017) 65–71, https://doi.org/10.1016/j.microrel.2017.07.087.
[5] S. Öztürk, P. Poşpoş, V. Utalay, A. Koç, M. Ermiş, I.J.S.E. Çadırcı, Operating principles and practical design aspects of all SiC DC/AC/DC converter for MPPT in grid-connected PV supplies, Sol. Energy 176 (2018) 380–394, https://doi.org/10.1016/j.solener.2018.10.049.
[6] N.C. Sintamarean, H. Wang, F. Blaabjerg, P.d.P.J.M.R. Rimmen, A design tool to study the impact of mission-profile on the reliability of SiC-based PV-inverter devices, Microelectron. Reliab. 54 (2014) 1655–1660, https://doi.org/10.1016/j.microrel.2014.07.055.
[7] Y. Chen, H.-Z. Huang, Y. Rao, Z. He, P. Lai, Y. Chen, X. Xu, C.J.M.R. Liu, Degradation assessment of 1.2-kV SiC MOSFETs and comparative study with 1.2-kV Si IGBTs under power cycling, Microelectron. Reliab. 132 (2022) 114528, https://doi.org/10.1016/j.microrel.2022.114528.
[8] M. Aditya, K.S.J.T.o.E. Rao, E. Materials, Design and performance analysis of advanced MOSFET structures, Transactions on Electrical and Electronic Materials 23 (2022) 219–227, https://doi.org/10.1007/s42341-021-00338-9.
[9] D.J.M.e. Vasileska, Modeling thermal effects in nano-devices, Microelectron. Eng. 109 (2013) 163–167, https://doi.org/10.1016/j.mee.2013.03.058.
[10] K. Heng, X. Yang, X. Wu, J. Ye, G. Liu, A temperature-dependent physical thermal network model including thermal boundary conditions for SiC MOSFET module, IEEE Trans. Electron. Dev. 69 (2022) 4444–4452, https://doi.org/10.1109/TED.2022.3185951.
[11] T. Kim, T. Funaki, Thermal measurement and analysis of packaged SiC MOSFETs, Thermochim. Acta 633 (2016) 31–36, https://doi.org/10.1016/j.tca.2016.03.004.
[12] H. Rezgui, F. Nasri, M.F.B. Aissa, A.A.J.T.S. Guizani, E. Progress, Investigation of nanoscale heat transport in sub-10 nm carbon nanotube field-effect transistors based on the finite element method, Therm. Sci. Eng. Prog. 25 (2021) 100938, https://doi.org/10.1016/j.tsep.2021.100938.
[13] J. Ghazanfarian, Z. Shomali, Investigation of dual-phase-lag heat conduction model in a nanoscale metal-oxide-semiconductor field-effect transistor, Int. J. Heat Mass Tran. 55 (2012) 6231–6237, https://doi.org/10.1016/j.ijheatmasstransfer.2012.06.052.
[14] M. Jamshidi, J. Ghazanfarian, Dual-phase-lag analysis of CNT–MoS2–ZrO2–SiO2–Si nano-transistor and arteriole in multi-layered skin, Appl. Math. Model. 60 (2018) 490–507, https://doi.org/10.1016/j.apm.2018.03.035.
[15] R. Hammer, V. Fritz, N. Bedoya-Martínez, M. Transfer, The worm-LBM, an algorithm for a high number of propagation directions on a lattice Boltzmann grid: the case of phonon transport, Int. J. Heat Mass Tran. 170 (2021) 121030, https://doi.org/10.1016/j.ijheatmasstransfer.2021.121030.
[16] O. Zobiri, A. Atia, M. Arıcı, A critical evaluation based on Lattice Boltzmann method of nanoscale thermal behavior inside MOSFET and SOI-MOSFET, Microelectron. J. (2021) 105191, https://doi.org/10.1016/j.mejo.2021.105191.
[17] A. Sohani, M. Dehbashi, F. Delfani, S. Hoseinzadeh, Optimal techno-economic and thermo-electrical design for a phase change material enhanced renewable energy driven polygeneration unit using a machine learning assisted lattice Boltzmann method, Eng. Anal. Bound. Elem. 152 (2023) 506–517, https://doi.org/10.1016/j.enganabound.2023.04.027.
[18] H. Wang, X. Hao, H. Zhou, Y. Zhang, D.J.M.E. Li, Underfill flow simulation based on lattice Boltzmann method, Microelectron. Eng. 149 (2016) 66–72, https://doi.org/10.1016/j.mee.2015.09.010.
[19] Y. Guo, M. Wang, Lattice Boltzmann modeling of phonon transport, J. Comput. Phys. 315 (2016) 1–15, https://doi.org/10.1016/j.jcp.2016.03.041.
[20] S. Kwon, M.C. Wingert, J. Zheng, J. Xiang, R. Chen, Thermal transport in Si and Ge nanostructures in the confinement regime, Nanoscale 8 (2016) 13155–13167, https://doi.org/10.1039/C6NR03634A.
[21] M.F.B. Aissa, H. Rezgui, F. Nasri, H. Belmabrouk, A. Guizani, Thermal transport in graphene field-effect transistors with ultrashort channel length, Superlattice. Microst. 128 (2019) 265–273, https://doi.org/10.1016/j.spmi.2019.02.004.
[22] M. Xu, H. Hu, A ballistic-diffusive heat conduction model extracted from Boltzmann transport equation, Proc. R. Soc. A 467 (2011) 1851–1864, https://doi.org/10.1098/rspa.2010.0611.
[23] F. Nasri, M.B. Aissa, H. Belmabrouk, Microscale thermal conduction based on Cattaneo-Vernotte model in silicon on insulator and Double Gate MOSFETs, Appl. Therm. Eng. 76 (2015) 206–211, https://doi.org/10.1016/j.applthermaleng.2014.11.038.
[24] F. Nasri, M.F.B. Aissa, M.H. Gazzah, H. Belmabrouk, 3D thermal conduction in a nanoscale Tri-Gate MOSFET based on single-phase-lag model, Appl. Therm. Eng. 91 (2015) 647–653, https://doi.org/10.1016/j.applthermaleng.2015.08.045.
[25] O. Zobiri, A. Atia, M. Arıcı, Study of robin condition influence on phonon nano-heat conduction using meso-scale method in MOSFET and SOI-MOSFET devices, Mater. Today Commun. 26 (2021) 102031, https://doi.org/10.1016/j.mtcomm.2021.102031.
[26] R. Yang, G. Chen, M. Laroche, Y. Taur, Simulation of nanoscale multidimensional transient heat conduction problems using ballistic-diffusive equations and phonon Boltzmann equation, J. Heat Tran. 127 (2005) 298–306, https://doi.org/10.1115/1.1857941.
[27] H. Rezgui, F. Nasri, M.F.B. Aissa, A.A. Guizani, in: IntechOpen (Ed.), Study of Heat Dissipation Mechanism in Nanoscale MOSFETs Using BDE Model, Green Electronics, 2018, p. 15, https://doi.org/10.5772/intechopen.75595.

Nomenclature

T: Temperature,K
T_0: ambient Temperature,K
R_{th}: thermal resistance
Kn: Knudsen number
ħ: Planck constant,Js
h: convective thermal coefficient
ν: Velocity,ms^{-1}
C: Volumetric heat capacity,$Jm^{-3}K^{-1}$
k: Thermal conductivity,$Wm^{-1}K^{-1}$
L_c: Channel length,m
k_B: Boltzmann constant,JK^{-1}
t: Time,s
x,y: Directions,m
g: Phonon energy density,Jm^{-3}
q_v: Heat generation Wm^{-3}
p: Specularity parameter

Abbreviations

PV: Photovoltaic
TJBC: Temperature Jump Boundary Condition
SiC: Silicon Carbide
BDE: Ballistic Diffusive Equation
IGPT: Insulated-gate Bipolar Transistor

Greek Letter

ω: Phonon frequency,s^{-1}
τ: Phonon relaxation time,s
θ: Debye temperature,K
Λ: Mean free path,m
η: Density of osillators,m^{-3}

Subscripts/Superscripts

eq: Equilibrium
**:* Dimensionless
w: Wall
i: Discrete direction